A Performance Comparison of two Time Diversity Systems using OS-CFAR Detection for Partially Correlated Chi-square Targets and Multiple Target Situations

[*]Toufik LAROUSSI and [**]Mourad BARKAT

[*]Département d'Electronique; Université de Constantine; Constantine 25000; Algeria.
Phone/Fax: 213-31-81-90-10. E-mail: toufik_laroussi@yahoo.fr

[**]Department of Electrical Engineering, American University of Sharjah, P. O. Box 26666, Sharjah, United Arab Emirates. Phone: 971-6-515-2932, Fax: 971-6-515-2979. E-mail: mbarkat@aus.edu

***Abstract* — In radar systems, detection performance is always related to target models and background environments. In time diversity systems, the probability of detection is shown to be sensitive to the degree of correlation among the target echoes. In this paper, we derive exact expressions for the probabilities of false alarm and detection of a pulse-to-pulse partially correlated target with 2K degrees of freedom for the Order Statistics Constant False Alarm Rate (OS-CFAR) detector. The analysis is carried out for the "non conventional time diversity system" (NCTDS) and multiple target situations. The obtained results are compared with the "conventional time diversity system" (CTDS).**

***Index Terms* — OS-CFAR detection, Time Diversity Systems, Conventional, Non conventional, Pulse-to-pulse correlation, Degrees of freedom**.

I. INTRODUCTION

In automatic detection, received signals might fade due to target fluctuations. According to Swerling's models, if only one pulse per scan hits a target, we cannot distinguish between cases I and II and cases III and IV. However, if multiple pulses are transmitted per antenna scan, the problem of detecting slow fluctuating targets (complete correlation) and fast fluctuating targets (complete decorrelation) can be easily overcome. Nevertheless, we should take into consideration the partial correlation of the target signal; otherwise the processor fails to predict the actual system performance. In other words, the more we know about the statistics of the target signal, the better the detection is.

In the literature of CFAR detection, the echoed signals of the transmitted pulses are processed non coherently within the same receiver. The non coherent integration accumulates M pulses and processes them as an entity to form the noise level estimate. Dealing with either uncorrelated or partially correlated data samples, we often seek to improve detection while maintaining a constant false alarm rate. Several authors have considered different applications of the non coherent integration. Here, we only list a few of them [1-5]. In [1], Kanter has studied the detection performance of a noncoherent integration detector accumulating M-correlated pulses from a Rayleigh target with two degrees of freedom. Complete correlation and complete decorrelation of the target returns yielding Swerling models I and II, respectively, were treated as extreme cases of the target correlation coefficient. The noise was assumed to be uncorrelated. Wiener [2] extended the work in [1] by deriving exact expressions for the probabilities of detection for partially correlated chi-square targets with four degrees of freedom. In this case, the limiting bounds of complete correlation and complete decorrelation of the target returns yield the Swerling models III and IV. The work done in [1, 2] used a fixed threshold detection. It is known that radar detectors with fixed threshold can not maintain a CFAR, and thus adaptive threshold detection is considered. Hou [3] used the method of residues to evaluate exact formulas for the detection performance for the chi-square family with 2K degrees of freedom.

The idea of processing independently the received target pulses to yield preliminary decisions in distributed CFAR detection, was first suggested by Himonas and Barkat [4, 5]. They studied the case of partially correlated target returns with different architectures of time diversity and distributed CFAR detectors to minimize the effect of the correlation factor among the received target pulses. They called it "time diversity systems" referring to multiple-pulse systems. El Mashade [6, 7] has thoroughly developed this idea by considering the integration of all the individual noise level estimates. More precisely, as shown in Fig. 1, the reference samples of the individual pulse returns are ranked in an ascending order. Then, each ordered window is processed by the suited one-pulse order-statistic algorithm. Finally, the obtained noise level estimates are added to get the overall background level. We call it "non conventional technique" with respect to the conventional non coherent integration technique. Consequently, for the sake of comparison, we shall adopt the terminology "conventional time diversity system" (CTDS) to refer to the non coherent integration and "non conventional time diversity system" (NCTDS) to refer to the technique used in [6, 7].

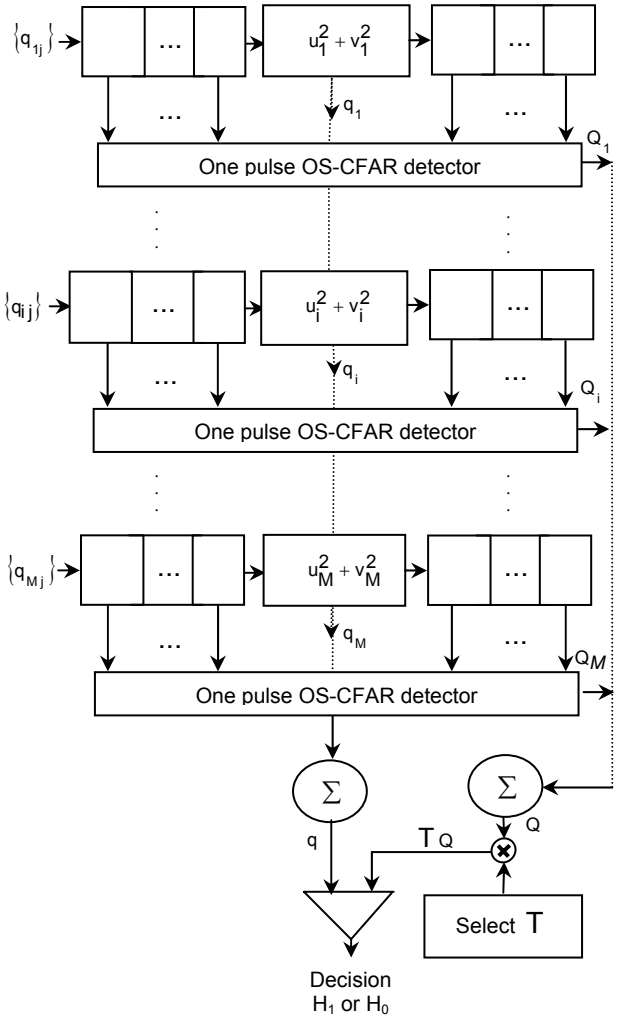

Fig. 1 Decision Element: NCTDS OS-CFAR detector

Of particular interest to radar applications is the presence of interfering targets in the reference cells, which is known to degrade the performance of CFAR detectors. To alleviate this problem, a lot of detectors have been proposed in the literature. The aim of these algorithms is to show how robust a CFAR detector can be in multiple target situations by taking into account the non homogeneity of the background either analytically or by simulation.

In summary, we observe that the work using the NCTDS did not show a comparison of the OS-CFAR detector with its corresponding detector for the CTDS in neither single nor multiple target situations. Moreover, the two systems did not consider the general case of a pulse-to-pulse partially correlated chi-square target with 2K degrees of freedom. To complete the study, we introduce a detailed detection analysis for a mathematical model representing the case of detecting a pulse-to-pulse chi-square partially correlated chi-square target with 2K degrees of freedom embedded in a pulse-to-pulse Rayleigh and uncorrelated thermal noise.

The paper is organized as follows. In Section 2, we formulate the statistical model. In Section 3, we derive the exact false alarm probability P_{fa}. Then, in Section 4, we give the moment generating function (mgf) of the test cell under hypothesis H_1 in terms of K and use it to derive the exact detection probability P_d. Next, in Section 5, by deriving detection curves, we show the performances of the detector. A conclusion is given in Section 6.

II. Statistical Model

The received signal is processed by the in-phase and quadrature phase channels. Assuming a correlated chi-square target with 2K degrees of freedom embedded in uncorrelated noise, the in-phase and quadrature phase samples $\{a_{ij}\}$ and $\{b_{ij}\}$ at pulse i and range cell j, respectively, i=1, 2, 3, …, M and j=1, 2, 3, …, N, are observations from Gaussian random variables. M and N are the number of radar processed pulses and the number of reference range cells, respectively. Assuming that the total noise power is normalized to unity, the output of the (i, j) [th] cell, is

$$q_{ij} = \frac{1}{2}\left\{a_{ij}^2 + b_{ij}^2\right\} \qquad (1)$$

The thermal noise samples are assumed to be independent and identically distributed (IID) random variables with zero mean and variance σ_n^2 (σ_n^2=1) from pulse-to-pulse and from cell-to-cell.

The detection performance is based upon the statistics of q, which is given by

$$q = \frac{1}{2}\sum_{i=1}^{M}\left\{u_i^2 + v_i^2\right\} \qquad (2)$$

Extending the target model introduced in [2] to 2K degrees of freedom, we have

$$u_i = x_i + a_i \text{ and } v_i = y_i + b_i, \quad i=1, 2,\ldots, M \qquad (3)$$

where $x_i = \sqrt{\sum_{k=1}^{K} x_{ik}^2}$ and $y_i = \sqrt{\sum_{k=1}^{K} y_{ik}^2}$ (i=1, 2, ..., M) are, respectively, the magnitudes of the in-phase and the quadrature phase components of the complex target signal at pulse i, present in the test cell q. x_i^2 and y_i^2 represents each the sum of the squares of K real Gaussian variables. K is called either the fluctuation parameter or the number of degrees of freedom. a_i and b_i represent the in-phase and quadrature phase samples of the uncorrelated thermal noise. The target signal is assumed to be independent from the thermal noise signal. The in-phase samples are assumed to be independent of the quadrature phase samples. A useful representation of the target signal vector, which will be used later in this paper, is

$$\mathbf{X} = \left[\mathbf{X}_1^T, \ldots, \mathbf{X}_K^T\right]^T \text{ and } \mathbf{Y} = \left[\mathbf{Y}_1^T, \ldots, \mathbf{Y}_K^T\right]^T \qquad (4)$$

where, $\mathbf{X}_k = [x_{1k}, \cdots, x_{Mk}]^T$, $\mathbf{Y}_k = [y_{1k}, \cdots, y_{Mk}]^T$ and k=1, 2,…, K . The M x 1 target in-phase vectors $\mathbf{X_1}$, $\mathbf{X_2}$,…, $\mathbf{X_k}$ and the quadrature phase vectors $\mathbf{Y_1}, \mathbf{Y_2}, \ldots, \mathbf{Y_k}$ are independent from each other but their respective components are correlated pulse-to-pulse. The K-block in-phase and quadrature phase target vectors **X** and **Y** of the correlated chi-square target model with 2K degrees of freedom are uncorrelated, but their respective components are correlated with a known correlation matrix $\mathbf{\Lambda_t}$. The random variables x_{ik} and y_{ik} (i=1, 2…, M) representing the target samples are assumed to be first-order Markov processes with zero mean and variance σ_t^2. Hence, the $(i,j)^{th}$ element of the covariance matrix of the target process $\mathbf{\Lambda_t}$ can be expressed as

$$[\mathbf{\Lambda}_t]_{i,j} = \begin{cases} \sigma_t^2 \, \rho_t^{|i-j|} & 0 < \rho_t < 1 \\ \sigma_t^2 \, \delta_{ij} & \rho_t = 0 \\ \sigma_t^2 \quad \forall i,j & \rho_t = 1 \end{cases} \tag{5}$$

According to Edrington's measurements, if M pulses hit a target, the return echoes from commonly encountered models are exponentially correlated. $\rho_t = \exp(-T_R \omega_t)$ is the correlation coefficient between the pulse-to-pulse received target samples for a given k where f_t is the mean Doppler frequency of the target signal. To simplify the analysis, we assume that the target process is stationary and that the pulse repetition interval (PRI) T_R is constant. Our model assumes that any value of $K \geq 1$ is realizable. The four Swerling cases (I, II) and (III, IV) correspond to K=1 and K=2, respectively. In this manner, we can model the partial correlation between pulses as in [1, 2]. Thus, for example, to model Swerling cases I and II, we should set K=1, but $\rho_t = 1$ and $\rho_t = 0$, respectively.

The test cell q is then compared to the adaptive threshold TQ to make a decision H_1 or H_0, according to the following hypothesis test

$$q \underset{H_0}{\overset{H_1}{\gtrless}} TQ \tag{6}$$

Q denotes the estimated background level, H_0 denotes the absence of a target while H_1 denotes the presence of a target. The probabilities of false alarm and detection of a CFAR detector can be obtained by using the contour integral [8], which can also be expressed in terms of the residue theorem as in [3] to yield

$$P_{fa} = \sum_{i_0} \text{res}\left[s^{-1} \Phi_{q|H_0}(s) \Phi_Q(-Ts), s_{i_0} \right] \tag{7}$$

$$P_d = \sum_{i_1} \text{res}\left[s^{-1} \Phi_{q|H_1}(s) \Phi_Q(-Ts), s_{i_1} \right] \tag{8}$$

where res [.] denotes the residue. s_{i_0} (i_0 = 1, 2, …) and s_{i_1} (i_1 = 1, 2, …) are, respectively, the poles of the moment generating function (mgf) $\Phi_{q|H_0}(s)$ of the noise and the mgf $\Phi_{q|H_1}(s)$ of the target plus noise, lying in the left-hand of the complex s-plane. $\Phi_Q(-Ts)$ is the mgf of the estimated background level evaluated at s= -Ts.

III. Evaluation of the False Alarm Probability

In order to derive the exact expression for the P_{fa}, we must evaluate the moment generating function (mgf) $\Phi_{q|H_0}(s)$ of the test cell q in the absence of a target and the mgf $\Phi_Q(s)$. As we stated earlier, the block diagram of the OS-CFAR integrating M pulses for the NCTDS is shown in Fig. 1. The mgf of q in the absence of a target is defined, in terms of the M x 1 noise vectors, as

$$\Phi_{q|H_0}(s) = \int_{-\infty}^{+\infty} \int_{-\infty}^{+\infty} p(\mathbf{A}, \mathbf{B}) \exp\left[-\frac{1}{2} s \left(|\mathbf{A}|^2 + |\mathbf{B}|^2 \right) \right] d\mathbf{A}\, d\mathbf{B} \tag{9}$$

As the in-phase and quadrature phase samples of the noise are IID, therefore the joint probability density function (pdf) of **A** and **B** satisfies $p(\mathbf{A}, \mathbf{B}) = p(\mathbf{A}) p(\mathbf{B})$ and $p(\mathbf{A}) = p(\mathbf{B})$. $p(\mathbf{A})$ is the joint Gaussian pdf of the in-phase noise vector with zero mean and identity covariance matrix which generates uncorrelated thermal noise samples [1]

$$p(\mathbf{A}) = \frac{1}{(2\pi)^{M/2}} \exp\left(-\frac{1}{2} |\mathbf{A}|^2 \right) \tag{10}$$

Combining equations (9) and (10) and after some mathematical manipulations, the mgf of the cell under test can be expressed as

$$\Phi_{q|H_0}(s) = (1+s)^{-M} \tag{11}$$

The poles of the mgf $\Phi_{q/H_0}(s)$ of q under hypothesis H_0 are a simple pole at $s = -1$ of multiplicity M lying in the left-hand s-plane.

The overall background noise level q is estimated by taking the average over the M pulses as follows

$$Q = \sum_{i=1}^{M} Q_i \tag{12}$$

The background noise level Q_i of the OS-CFAR detector is estimated by the n^{th} ranked sample taken among the N ordered cells [9] as

$$Q_i = q_{i(n)} \qquad i=1, 2, \ldots, M \tag{13}$$

Note that the value of n is the same for all processed pulses. It is shown that the best performance of the OS CFAR detector in multiple target situations is obtained for $n = 3N/4$. As the mgf of Q_i for i=1, 2, …, M is given in [8] and assuming that the Q_i's are IID from pulse-to-pulse, then the mgf of Q is

$$\Phi_Q(s) = \prod_{l=1}^{n} (1 + a_l\, s)^{-M} \qquad (14)$$

where, $a_l = (N - l + 1)^{-1}$

The P_{fa} of the OS-CFAR detector can be evaluated by substituting equations (11) and (14) for s = -T s into equation (7). Then by using the partial-fraction expansion, we obtain

$$P_{fa} = -\frac{1}{\Gamma(M)} \prod_{l=1}^{n} (-T\, a_l)^{-M} \frac{d^{M-1}}{ds^{M-1}} \left[\frac{1}{s} \left(\sum_{l=1}^{n} \frac{k_l}{s - s_l} \right)^{M} \right]_{s=-1} \qquad (15)$$

$$\Gamma(M) = (M-1)!,\ k_l = \prod_{\substack{i=1 \\ i \neq l}}^{n} (a_l - a_i)^{-1} \text{ and } s_l = (T a_l)^{-1}$$

IV Evaluation of the Detection Probability

Now let us derive the exact expression for the detection probability. In doing this, we study the effect of the correlation coefficient ρ_t of the target returns on the detection performance. The determination of the P_d given by equation (8) requires the knowledge of the $\text{mgf}\,\Phi_{q/H_1}(s)$ of the test statistic q under H_1 and the $\text{mgf}\,\Phi_Q(s)$ of the background noise level Q of the OS-CFAR detector.

Taking into account that **X** and **Y** are independent, **A** and **B** are independent and that the noise signal is Gaussian, stationary and independent of the target signal, we can write the mgf of q in the presence of the target for any target model [2, as Eq. (7)], as

$$\Phi_{q|H_1}(s) = \frac{1}{(1+s)^M} \left[\int_{-\infty}^{+\infty} p(\mathbf{X}) \exp\left(-\frac{s|\mathbf{X}|^2}{2(1+s)} \right) d\mathbf{X} \right]^2 \qquad (16)$$

The target K-bloc vector $\mathbf{X}$ as defined in equation (4), has a multivariate Gaussian pdf, defined by

$$p(\mathbf{X}) = \frac{1}{(2\pi)^{KM/2}\, |\mathbf{\Lambda}|^{1/2}} \exp\left(-\frac{1}{2} \mathbf{X}^T \mathbf{\Lambda}^{-1} \mathbf{X} \right) \qquad (17)$$

The K x K block diagonal covariance matrix $\mathbf{\Lambda}$ is defined as

$$\mathbf{\Lambda} = \text{diag}\ (\mathbf{\Lambda}_t, ..., \mathbf{\Lambda}_t) \qquad (18)$$

Note that since $\mathbf{\Lambda}_t^{-1}$ exists then, $\mathbf{\Lambda}^{-1}$ also exists.

In order to find the mgf of the test statistic under H_1, we need to evaluate equation (16). That is, we first define the pdf of the vector X_k, k=1, 2, …, K, as in [2]

$$p(\mathbf{X_k}) = \frac{1}{(2\pi)^{M/2}\, |\mathbf{\Lambda}_t|^{1/2}} \exp\left(-\frac{1}{2} \mathbf{X}_k^T \mathbf{\Lambda}_t^{-1} \mathbf{X}_k \right) \qquad (19)$$

Since the M x 1 target in-phase vectors $X_1, X_2, \ldots, X_k$ and quadrature phase vectors $Y_1, Y_2, \ldots, Y_k$ are independent from each other, we introduce the pdf of the K-dimensional vector $\mathbf{X}$ as a generalization of [2, as Eq. (10)]

$$p(\mathbf{X})\, d\mathbf{X} = \prod_{k=1}^{K} p(\mathbf{X}_k)\, d\mathbf{X}_k \qquad (20)$$

From equation (4), we define also the norm of the vector $\mathbf{X}$, i.e. $|\mathbf{X}|^2$ as

$$|\mathbf{X}|^2 = \sum_{k=1}^{K} \mathbf{X}_k^T \mathbf{X}_k \qquad (21)$$

Inserting equation (17) into (16) and integrating over the X_k's, we may write, by using equations (18) to (21)

$$\Phi_{q|H_1}(s) = \frac{(1+s)^{M(K-1)}}{\left| \mathbf{I} + (\mathbf{I} + \mathbf{\Lambda}_t) s \right|^K} \qquad (22)$$

If the target signal is assumed to be a stationary process, then $\mathbf{\Lambda}_t$ is a symmetric Toeplitz matrix with M distinct positive real eigenvalues denoted by β_i, i=1, 2, …, M. Therefore, the determinant which appears in (22) may be expressed as the product of its eigenvalues.

$$\Phi_{q_0|H_1}(s) = \frac{(1+s)^{M(K-1)}}{\prod_{i=1}^{M} [1 + (1 + \beta_i) s]^K} \qquad K=1, 2, 3, \quad (23)$$

Note that the mgf of [3] given for chi-square targets with 2K degrees of freedom, is a special case of the mgf given by equation (23) for partially correlated chi-square target with 2K degrees of freedom.

The P_d of the OS-CFAR detector can be found by inserting equations (14) for s = -T s and (23) into equation (8). Then by using the partial-fraction expansion, we get

$$P_d = -\frac{\alpha}{\Gamma(K)} \sum_{i=1}^{K} \gamma_i \frac{d^{K-1}}{ds^{K-1}} \left[\frac{(1+s)^{M(K-1)}}{s} \left(\sum_{\substack{j=1 \\ j \neq i}}^{M} \frac{k_j}{s - s_j} \right)^K \left(\sum_{l=1}^{n} \frac{k_l}{s - s_l} \right)^M \right]_{s=s_i} \qquad (24)$$

where, $\Gamma(K) = (K-1)!$, $\alpha = \prod_{l=1}^{n} (-T\, a_l)^{-M}$,

$$\sigma_i = (1 + \beta_i)^{-K},\ k_j = \prod_{\substack{n=1 \\ n \neq j \\ n \neq i}}^{M} (b_j - b_n)^{-1} \text{ and } \gamma_i = \sigma_i \prod_{\substack{j=1 \\ j \neq i}}^{M} (1 + \beta_j)^{-K}$$

V. Simulation Results

To evaluate the detection performance and the false alarm properties of the proposed model, we assume a reference window size of N=16 and design $P_{fa}=10^{-4}$. First, we compute the threshold multiplier T of the OS-

CFAR detector (n=12) for the NCTDS using equation (15) to achieve the prescribed P_{fa}. Then, for the same assigned P_{fa}, we obtain by simulation the threshold multiplier of the corresponding detector for the CTDS. The P_d for the NCTDS is computed using equation (24) while the P_d for the CTDS is obtained by simulation. In both cases, the detection performance of the detector for a design P_{fa}, depends upon several parameters. Our attention is focused on the signal-to-noise ratio (SNR), the target correlation coefficient ρ_t, the number of processed pulses M and the number of degrees of freedom K with an emphasis on the problem of multiple target situations.

In the absence of interfering targets, Fig. 2 shows the probability of detection against SNR. We can observe from this figure that there is a complete overlap of the curves representing the CTDS and the NCTDS. Note that a target correlation going from $\rho_t = 1$ to $\rho_t = 0$ helps the detection. The greater the K, the more insensitive to ρ_t the detection becomes. The Swerling's cases are the extreme limits represented by $\rho_t = 1$ representing complete correlation of the target, and $\rho_t = 0$ representing complete decorrelation.

In all forthcoming experiments, we assume that more than one target may be present. They are all of the same nature (primary and secondary targets). The interference-to-noise ratio is noted INR and we assume that INR=SNR. For the same conditions as above, we add four interferers. Inspection of Fig. 3 reveals that the detector is more sensitive to the presence of interfering targets for the NCTDS than for the CTDS. The CFAR loss between the two systems becomes more significant when K increases.

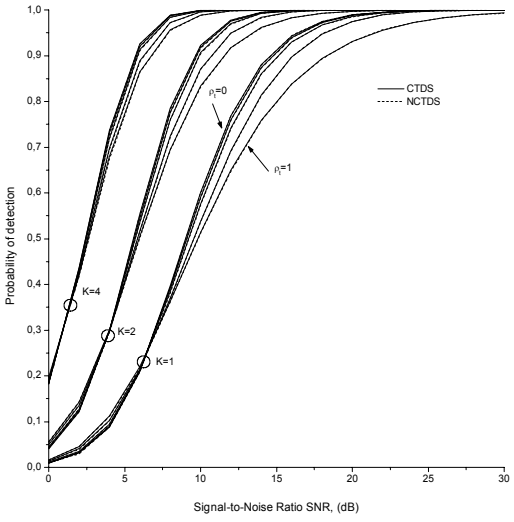

Fig. 2 Probability of detection of the CTDS and the NCTDS OS-CFAR detector against SNR in the absence of interfering targets for N=16, ρ_t=0, 0.3, 0.5, 0.8 and 1, NI=0, M=2 and $P_{fa}=10^{-4}$.

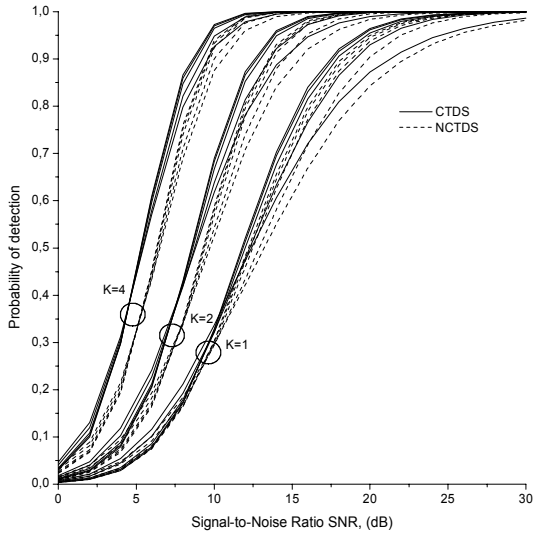

Fig. 3 Probability of detection of the CTDS and the NCTDS OS-CFAR detector against SNR for N=16, ρ_t=0, 0.3, 0.5, 0.8 and 1, NI=4, M=2 and $P_{fa}=10^{-4}$.

Next, we examine the effect of ρ_t, and the number of interferers (NI), respectively, on the detectability of correlated chi-square targets with 2K degrees of freedom at SNR=INR=5dB for the same N and the same P_{fa}. We observe in Figs. 4 and 5 that in the absence of interferers, the detector for the two considered systems, CTDS and NCTDS, have the same performance. The presence of multiple interferers affects more the detector for the NCTDS than the corresponding detector for the CTDS. This is primarily due to the fact that the spikes present in the individual reference cells are compensated from one pulse to another with the flats present in the corresponding cells. The CTDS takes then full advantage of this compensation mechanism as the number of interfering targets increases. As expected, the OS-CFAR detector for the two systems becomes vulnerable when the number of interferers exceeds four. This agrees with the results obtained for the one pulse detector treated in [8]. Nevertheless, the detector performs better for the NCTDS than for the CTDS. In Fig. 4, we plot the P_d for the two systems in terms of ρ_t. As it is well-known, an increase in the target correlation coefficient degrades the detection for all kind of detectors. The case NI=5 indicates that the detector for both systems can not handle anymore interfering targets.

To investigate more interesting operational cases, we test the robustness of the detector in the presence of multiple interfering targets in the range cells. Fig. 5 shows the P_d in terms of NI. Note that, although the detector for the CTDS for which the detection degrades seriously for NI $\geq$ 5, independently of the number of processed pulses M, the corresponding detector for the NCTDS degrades smoothly. Finally, observe that when

M is sufficiently large, the detection improves significantly for a moderate NI.

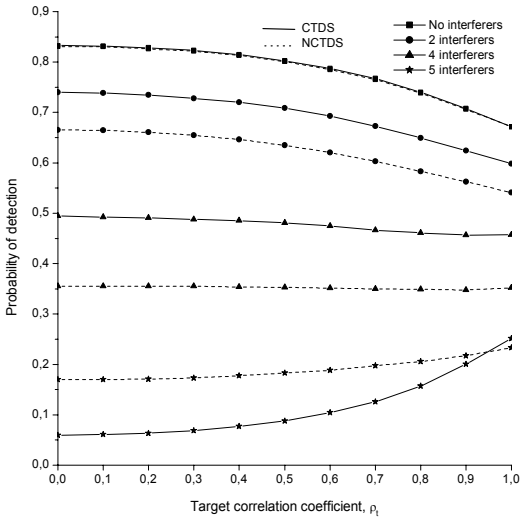

Fig. 4 Probability of detection of the CTDS and the NCTDS OS-CFAR detector against Target correlation coefficient at SNR=5dB for K=2, N=16, M=4, INR=SNR and $P_{fa}=10^{-4}$.

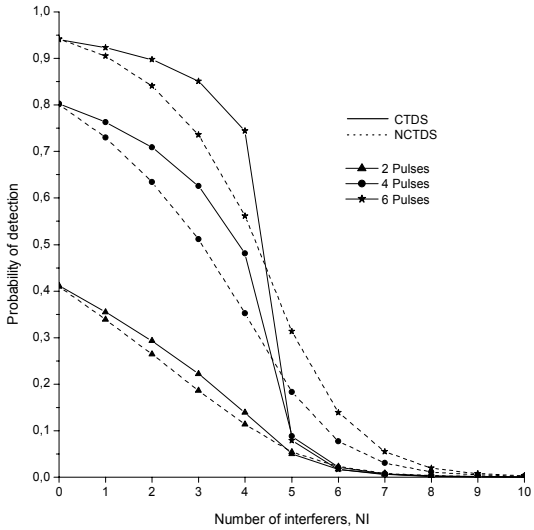

Fig. 5 Probability of detection of the CTDS and the NCTDS OS-CFAR detector against Number of interferers at SNR=5dB for K=2, N=16, ρ_t =0.5, INR=SNR and $P_{fa}=10^{-4}$.

VI. Summary and Conclusion

In this paper, we analyzed and compared the performance of the OS-CFAR detector using two different noncoherent integration systems for the detection of a pulse-to-pulse partially correlated target with 2K degrees of freedom immersed in a pulse-to-pulse Rayleigh uncorrelated noise and multiple target situations. The obtained results showed that their performance are very similar in the absence of interfering targets, in which case the simple mathematics induced by the NCTDS makes it a good alternative since the problem of large processing time required can be easily overcome by using new generation high speed processors. When the number of interferers does not exceed the number of trimmed samples and due to its compensation mechanism, the CTDS is more robust than the NCTDS. However, for more interferers, the NCTDS exhibits better detection performance.

References

[1] I. Kanter, 'Exact detection probability for partially correlated Rayleigh targets', *IEEE Transactions on Aerospace and Electronics Systems*, AES-22, (2), Mar. 1986, pp. 184-196.

[2] M. A. Weiner, 'Detection probability for partially correlated chi-square targets' IEEE Transactions on Aerospace and Electronics Systems, 24, July 1988, pp. 411-416.

[3] Hou Xiu-Ying, 'Direct evaluation of radar detection probabilities', *IEEE Transactions on Aerospace and Electronics Systems*, vol. AES-23, NO. 4, July 1987, pp. 418-423.

[4] S. D. Himonas and M. Barkat, 'On CFAR detection of correlated radar signals', *Proceedings of the 28th Conference on Detection and Control*, Tampa, Florida, Dec. 1989, pp. 1773-1778.

[5] S. D. Himonas and M. Barkat, 'A distributed CFAR processor with data fusion for correlated targets in nonhomogeneous clutter', *Proceedings of the International Radar Conference*, Washington, DC, 1990, pp. 501-506.

[6] M. B. El Mashade, 'Detection performance of the trimmed-mean CFAR processor with noncoherent integration' IEE Proceedings on Radar, Sonar and Navigation, Vol. 142, No. 1, Feb. 1995, pp. 18-24.

[7] M. B. El Mashade, 'Detection analysis of linearly combined order-statistic algorithms in nonhomogeneous background environments', *Signal Processing* 68, 1998, pp. 59-71.

[8] J. A. Ritcey, 'Calculating Radar Detection Probabilities by Contour Integration', *Ph. D. Dissertation*, Dept. of Electrical Engineering, University of California, San Diego, 1985.

[9] H. Rohling, 'Radar CFAR thresholding in clutter and multiple target situations', *IEEE Transactions on Aerospace and Electronics systems*, AES-19, July 1983, pp. 608-621.

[10] M. Barkat, *Signal Detection and Estimation*, Second Edition, Artech House, Boston, MA, September 2005.